



# Response evaluation of AA8011 with nano ZrB<sub>2</sub> inclusion for multifunctional applications: Considering its thermal, electrical, and corrosion properties



J. Fayomi <sup>a, b, c, \*</sup>, A.P.I. Popoola <sup>a, b</sup>, O.M. Popoola <sup>c</sup>, O.S.I. Fayomi <sup>a, b, d</sup>, E. Ajenifuja <sup>a, e</sup>

<sup>a</sup> Department of Chemical, Metallurgical and Materials Engineering, Tshwane University of Technology, P.M.B. X680, Pretoria, South Africa

<sup>b</sup> Surface Engineering Research Laboratory, Tshwane University of Technology, P.M.B. X680, Pretoria, South Africa

<sup>c</sup> Centre for Energy and Electric Power, Department of Electrical Engineering, Tshwane University of Technology, P.M.B. X680, Pretoria, South Africa

<sup>d</sup> Department of Mechanical Engineering, Covenant University, P.M.B. 123, Ota, Nigeria

<sup>e</sup> Centre for Energy Research and Development, Obafemi Awolowo University, Nigeria

## ARTICLE INFO

### Article history:

Received 1 September 2020

Received in revised form

12 September 2020

Accepted 13 September 2020

Available online 28 September 2020

### Keywords:

Stir casting

AA8011-ZrB<sub>2</sub>

Aluminium metal matrix composites

Thermal

Electrical

Corrosion

## ABSTRACT

Researches have shown severally that AA8011 alloy is limited in its multifunctional applications notwithstanding its intrinsic properties. Nevertheless, these properties can be improved by complementing with high-grade reinforcement that have better Performance characteristics. In this investigation, AA8011 properties are improved by ZrB<sub>2</sub> inclusion through a two-step stir casting process to enhance the thermal and corrosion resistance without significantly affecting the electrical properties. The thermal behaviour was analyzed using a thermogravimetric analyzer (TGA) and differential thermal analyzer (DTA), the corrosion response was studied with auto lab potentiodynamic polarization in 3.5% NaCl, the surface degradation after corrosion was observed with scanning electron microscope (SEM), and the electrical performance was carried out on the four-point probe meter. From the experiments, a decrease in the composite mass loss; improved melting temperature of about 674.4 C in the presence of ZrB<sub>2</sub> addition as a function of the temperature rise was achieved by TGA and DTA respectively. The high corrosion resistance of 7831.7 Ω and low corrosion rate of 0.5017 mm/yr at AA8011-20 wt% ZrB<sub>2</sub> was obtained, this was characterized by little or no visible pitting corrosion as revealed by SEM. The enhancement of the thermal stability and the improvement of the corrosion resistance prowess of AA8011 without an obvious compromise on its electrical behaviour is an indication that AA8011-ZrB<sub>2</sub> composite is a novel composite material for multifunctional application mostly where improved aluminium alloys are required.

© 2020 Elsevier B.V. All rights reserved.

## 1. Introduction

Aluminium and its alloys have overtime proven to be a good material of thermal and electrical conductivity, and the conductive properties are twice that of the steel. This has distinguished aluminium to be one of the most essential light materials used in power transmission, automobile radiator, residential utensils, and as the heat exchanger [1–3].

Notwithstanding its intrinsic properties, researches have shown that there is a high possibility of dislocation movement and

deformation induced by the light aluminium material as a function of the load applied, high temperature, and exposure to highly prone corrosion condition which in a way decreases the strength mechanism of the material, lower the thermal stability, and increases the pitting corrosion [4–6]. Hence, the need to improve the associated structural limitations becomes inevitable by multifunctional industries that require material of high thermal stability and strong resistance to corrosion attack in a deteriorated environment. Studies have affirmed that high-temperature resistance and high melting temperature of ceramics play a significant role in improving the low thermal stability of aluminium. This assertion was attested by Fayomi & Popoola (2019) [7], the authors reinforced AA8011 with Si<sub>3</sub>N<sub>4</sub> + ZrB<sub>2</sub> hybrid ceramic particulates to examine the response of the composite to the temperature. TGA and DTA

\* Corresponding author. Department of Chemical, Metallurgical and Materials Engineering, Tshwane University of Technology, P.M.B. X680, Pretoria, South Africa.  
E-mail addresses: [fayomi\\_chris@yahoo.com](mailto:fayomi_chris@yahoo.com), [218749836@tut4life.ac.za](mailto:218749836@tut4life.ac.za) (J. Fayomi).

were employed to evaluate the weight change of the material and the phase transformation as a function of temperature. The result of their TGA finding shows a decrease in material weight loss with an increase in ceramic reinforcement and the composite with 20% reinforcement shows the least weight loss. The DTA revealed that the incorporation of the Nanoceramic particulates increases the solid-liquid transformation of the developed composite compared to the unreinforced AA8011 alloy.

The reinforcement, mostly ceramics that are introduced into the primary light material acted as a load-bearing capacity thereby reducing the site of dislocation movement during [8]. This reinforcement substance often increases the stability and the strength of the developed composite as affirmed by Ref. [9–12]. Likewise, the corrosion resistance of aluminium alloys is well improved by the incorporation of the ceramics. The inert insulating nature of the ceramics filled the pore space in the matrix aluminium thereby blocking the possible site in which the infiltration of the negatively charged ion can occur.

The adoption of the aluminium based composite by the manufacturing industries has recently gained more popularity as a result of its ability to complement the existing properties of the light materials without compromising their phenomenon. The fabricated composite of the aluminium base has been found to have excellent corrosion resistance, improved mechanical strength with endowed stability at high temperatures. These improved structural properties have been made possible by the inclusion of the reinforcing ceramic material viz; borides, carbides, nitrides, and oxides of metals or transition metals [13–16]. However, the introduction of some inorganic ceramic substances as a means of improving the properties of a light metal sometimes resulted in high detriment to the intrinsic nature of such ductile materials. This is an indication that not all ceramic substituents can enhance a base material without causing more mayhems on their structural behaviour. Hence, proper consideration(s) is essential in choosing the best ceramic substituent based on the area of the demanding application.

The inclusion of boride-based ceramic such as TiB<sub>2</sub>, AlB<sub>2</sub>, ZrB<sub>2</sub> has been greatly employed to improve the properties of the light alloys of aluminium. The ability to enhance the alloy material without deteriorating or defecting their inherent nature has substantially distinguished this class of ceramic among other ceramic materials and position them as a leading material used in most industries to improve the light alloys. ZrB<sub>2</sub> especially, has been identified with high melting temperature, good corrosion resistance, and excellent strength mechanism due to their strong covalent Zr–B bonding [17–20].

Commercially, the manufacturing of aluminium-based composites often encounters some challenges during the fabrication processes. These limitations vary with the types of techniques employed to develop the composite. Usually, the cost of producing the composite, the complexity of the process route, and the possibility of achieving a defect-free composite are some of the barriers encountered in composite industries. How be it, two-step stir casting route among other techniques of developing composite remains the most popular and highly utilized method of fabricating composite owing to its flexibility, permissible act of large production, cost-effectiveness, and the ability to achieve a defect-free material by adjusting the parametric processes [21–23].

In summary, this research is conceptualized to study the thermal, corrosion, and electrical behaviour of AA8011 reinforced with nano ZrB<sub>2</sub> inclusion for multifunctional application.

## 2. Materials and methods

### 2.1. Materials

Commercially AA8011 ingots of the composition in Table 1 were utilized as the alloy base material for this study. Inorganic ceramic

ZrB<sub>2</sub> of size 50 nm was employed as the reinforcing substituents.

### 2.2. Methods

#### 2.2.1. AA8011-ZrB<sub>2</sub> composite fabrication

“The development of the binary composite of AA8011-ZrB<sub>2</sub> entails the use of a two-step stir casting route conducted in accordance with [24]. The fabrication process commences with the quantifying of the ZrB<sub>2</sub> particles and the base material AA8011 needed to formulate composite with 5 wt%, 10 wt%, 15 wt%, and 20 wt% reinforcement. The Nano ceramic ZrB<sub>2</sub> particulate was initially conditioned to remove unwanted impurities, exit moisture, and degas the surface layer to enhance wettability with the AA8011 melt at a temperature of 450 C. The representative pieces of AA8011 were introduced into the furnace and heated to 800 C above the melting temperature of the AA8011 alloy and then the molten alloy cool down in the furnace to a semi liquidus state before charging the preheated ZrB<sub>2</sub> into the melt pool of the alloy. The preheated particulates were introduced into the melt pool of AA8011 and the slurry was stirred manually for 5 min and then heated at a temperature of 800 C again. A mechanical stirrer was introduced into the slurry and stir at 300 rpm for about 10 min to enhance the uniform dispersion of the particulate in the melt pool of AA8011. The developed molten composite was then tilted into the sand mold for complete solidification before machining and other metallographic processes” [25].

The developed composite admixture is presented in Table 2.

#### 2.2.2. Thermal properties

The thermal behaviour of the developed aluminium metal matrix composites (AMMCs) was evaluated using a thermal gravimetric analyzer. The thermal analyses were carried out using PerkinElmer Thermal gravimetric analyzer (TGA 4000) in a nitrogen environment from 30 C to 900 C. The equipment measures the thermal stability of the AMMCs by recording the weight change during the exposure time. The specimens under test were suspended in a mullite tube inside a tubular furnace where the temperature is carefully examined with the temperature sensor. The data collected through thermogravimetric in a thermal reaction is compiled and used to plot a graph of mass on the y-axis against temperature on the x-axis. This plot is referred to as the TGA curve.

Also, the solid-liquid transition of the developed composites was analyzed using NETZSCH DTA 404. This analyzer evaluates the evolutionary change of material as a function of the heating temperature in a controlled environment.

#### 2.2.3. Electrical properties

The electrical behaviour of the developed composite was analyzed by employing a four-point probe meter (Hp2662, China)

**Table 1**  
Chemical composition of AA8011.

Fe 0.665	Si 0.484	Mn 0.071	Cu 0.114	Zn 0.200
Ti 0.012	Mg 0.463	Pb 0.008	Sn 0.012	Al 97.90

**Table 2**  
Experimental design for the composite development.

Sample	AA8011 (wt.%)	ZrB <sub>2</sub>
V	100	0
W	95	5
X	90	10
Y	85	15
Z	80	20

with a constant current of 100 mA. For every analysis on the 20 × 20 mm samples, the device was auto zeroed before commencing the reading of the resistivity. The electrical conductivity was inversely gotten from the value of resistivity.

2.2.4. Corrosion Properties

The anti-corrosion behaviour of the developed AMMCs in the simulated 3.65% NaCl was analyzed using a linear potentiodynamic polarization method. Three (3) electrode system was employed to check the corrosion rate (mm/yr), corrosion potential (V), polarization potential (Ω), and current density (A/cm<sup>2</sup>). The current was fixed at 10 nA and 10 mA, the potential was regulated between -1.5 V and +1.5 V at a scan rate of 0.0015 V/s according to the ASTM G102-89, while the investigations were carried out using auto lab potentiostat coupled with NOVA software of 2.1 version.

The surface degradation of AA8011-ZrB<sub>2</sub> composite as a result of the corrosion attack after the electrochemical process was investigated using SEM VEGA 3 TESCAN, Czech Republic.

3. Results and discussion

3.1. Thermal behaviour of AA8011-ZrB<sub>2</sub> composite

Fig. 1 presents the TGA plots of the AA8011-ZrB<sub>2</sub> reinforced with different weight composition at a heating rate of 20 C/min from 30 °C to 900 °C. The curves revealed the thermal response of the unreinforced alloy and the reinforced composite having a similar profile with different percentages of reinforcement in an inert nitrogen environment. From the plots, the unreinforced as-cast AA8011 shows the onset temperature of degradation at 180 C, but the temperature gets improved by the addition of ZrB<sub>2</sub>. For example, 5 wt% of AA8011-ZrB<sub>2</sub> present the temperature of degradation at 220 C higher than the unreinforced alloy but lower than the 10 wt% with 270 C. The composite with 20 wt% ZrB<sub>2</sub> possessed the best onset temperature of decomposition at about 605 C which depicts a more thermally stable material.

Likewise, the effect of the mass-loss rate as a function of the

temperature to ascertain the behaviour of the material at different temperature degradation was examined. The incorporation of the ZrB<sub>2</sub> into the melt pool of the AA8011 decreases the rate of mass loss of the composite. As the percentage weight fraction of ZrB<sub>2</sub> increases from 0%, 5%, 10%,15%, to 20%, the mass loss decreases accordingly. The unreinforced alloy possessed 0.26 mg loss which is about 37.5% total mass loss, the addition of 5 wt% gives a reduced mass loss rate of 19.8%, 10 wt% gives 16.7%, and the best material loss decrement occurs at 20 wt% with 11.5%. The TGA curves demonstrated that the degree of mass misfortune, the temperature of decomposition and degradation depends on the percentage proportion of the reinforcement phase [26]. Affirmed that the increase in the temperature of decomposition could be ascribed to the barrier diffusion effect of the fickle decomposed material. Also, the loss in weight of the unreinforced alloy at high-temperature environments depicts poor thermal stability due to the free diffusion of decomposing material [27,28].

It is noteworthy to state that the inorganic hard nano ZrB<sub>2</sub> function as a blocking hurdle that is activated in the direction through which the product from the thermal decomposition could diffuse. Hence, the more the weight percentage of the nano reinforcement, the better enhanced the protection against material mass loss. This was responsible for the minimal mass loss recorded at 20 wt % with higher potential for thermal stability. According to Ref. [29], strong adhesive bond interactions that exist between a primary ductile AA8011 and the strong ceramic reinforcement were responsible for the thermal stability and the stability persisted with a percentage rise in the nano inclusion. The authors' assertion was reached when they investigated the thermal behaviour of the AA8011-Si<sub>3</sub>N<sub>4</sub> composite.

Fig. 2 shows the DTA curve of the developed AA8011-ZrB<sub>2</sub> with varying reinforcement weight proportion at a heating rate of 20 C/min from 30 C to 700 C. The curve shows that all the reinforced composite has higher melting temperatures (endothermic peak) compared to the unreinforced alloy. The most improved melting temperature (T<sub>m</sub>) was observed with 20 wt % ZrB<sub>2</sub> which had T<sub>m</sub> of 674.4 C above that of the AA8011. Hence, the material with 20 wt %

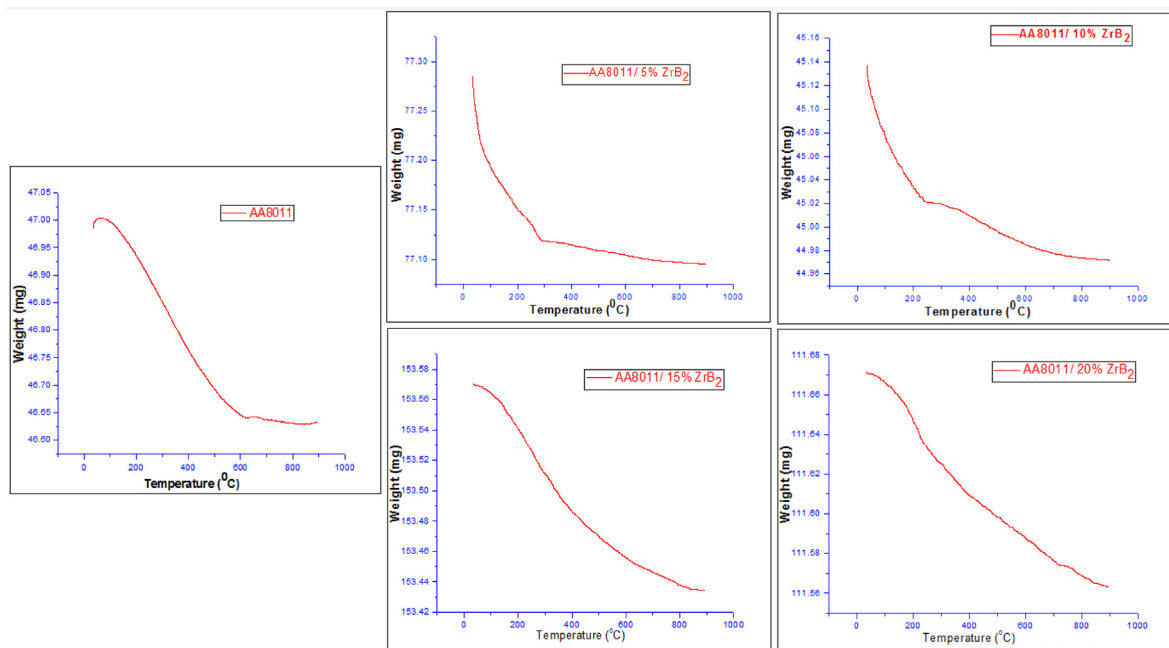


Fig. 1. Thermogravimetric analysis (TGA) results of the developed AA8011-ZrB<sub>2</sub> composite.

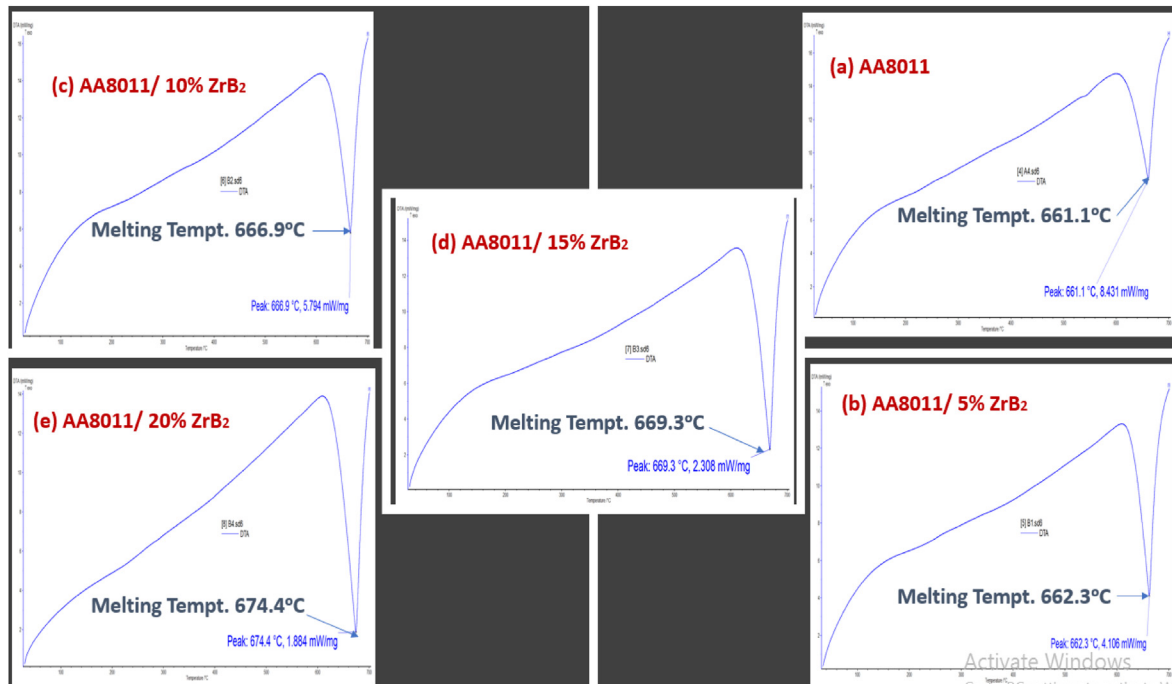


Fig. 2. The phase transformation of the developed AA8011-ZrB<sub>2</sub> composite by DTA

ZrB<sub>2</sub> was seen to be more thermally stable at high temperature. This is in an indication that the presence of the nano reinforcing phase has helped to block the sites (nano-pores and or micro-cracks) in which material loss can easily occur as a function of high temperature thereby enhancing the developed composite with prowess to withstand an environment or application with characterized high temperature.

In a nutshell, it is expedient to state that both TGA and DTA curves display a negligible mass loss of material on the developed composite with harnessed T<sub>m</sub>.

### 3.2. Electrical behaviour of the developed AA8011-ZrB<sub>2</sub> composite

The ZrB<sub>2</sub> weight content in the developed AA8011-ZrB<sub>2</sub> was varied from 5 wt% to 20 wt% in a stepwise of 5. In this research, the presence of the non-conductive nano ZrB<sub>2</sub> reduces the inherent electrical conductivity of the highly conductive AA8011 and the regression continues with the percentage rise in the nano inclusion as seen in Fig. 3. The highly conductive non-ferrous AA8011 metal was observed with  $2.34 \times 10^5$  S/m (40.28% IACS), this decreases to  $2.32 \times 10^5$  S/m (40.10% IACS) for the 5 wt% nano inclusion and the lowest electrical conductivity of  $2.26 \times 10^5$  S/m (39.01%) was experienced by 20 wt% ZrB<sub>2</sub>. Many factors are responsible for the decrease in the electrical conductivity of the composite viz; nature of the particulate inclusion, weight composition, reinforcement size and shape, and the type of adhesive bonding interaction that exists between the continuous and the discontinuous inter-phase [30]. Naturally, the inorganic ZrB<sub>2</sub> ceramic material is characterized by minimal electrical conductivity and its function as an insulator. Hence, the incorporation of such material often hinders the free flow of the active electron that influence the high conductivity of the AA8011 matrix thereby resulting to decrease in the electrical conductivity of the composite. Inversely, the electrical resistivity of the developed composite increases as a result of the degree of the electron distortion caused by the nano inclusion of ZrB<sub>2</sub>. As shown in Fig. 3, the highest resistivity of  $4.42 \times 10^{-6} \Omega\text{m}$

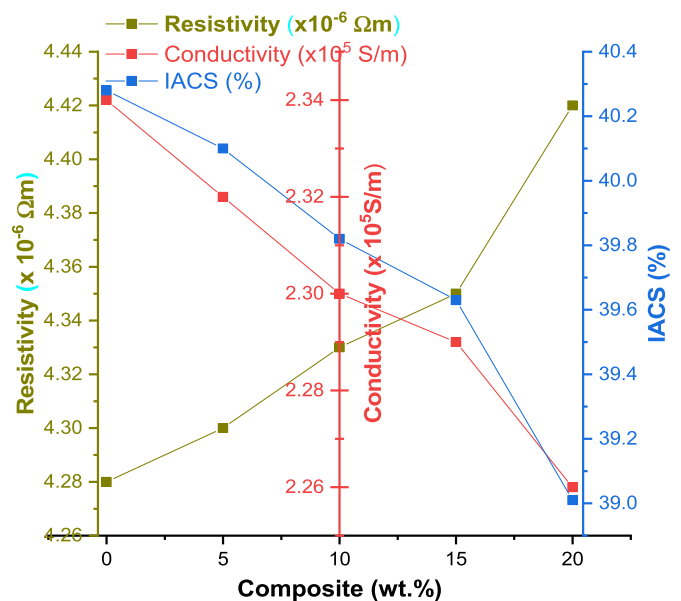


Fig. 3. Curves of the electrical properties of the developed composite.

for 20 wt% ZrB<sub>2</sub> was observed. Achieving wettability (defect-free structure) and uniform dispersion of nano ceramic inclusion during the fabrication process is essential as this helps to reduce the potency of electron scattering in the conductive continuous matrix phase. Usually, high porosity aids large distortion of electron movement and this invariably resulted in high resistivity. Hence, the lesser the micro-defect (porosity) in a material, the lower the resistivity. According to Ref. [29,31], the uniform distribution of the nonconductive material in the conductive matrix interface with a negligible defect location will aid the reduction in electron scattering and thereby reduce the resistivity value.

Generally, the overall minimum decrease in the conductivity of

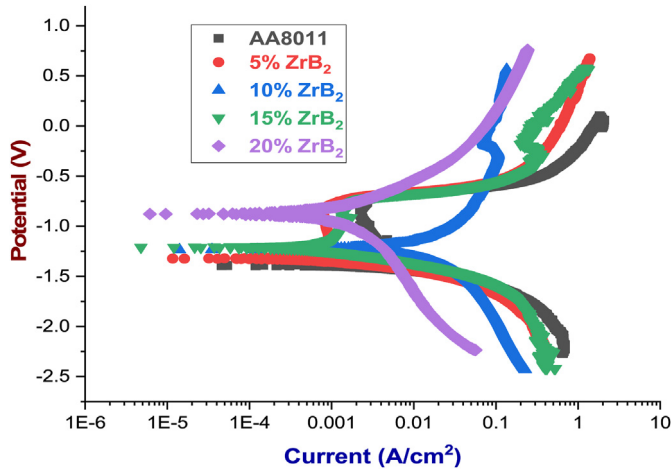


Fig. 4. Corrosion plots of the developed composite in NaCl.

the AA8011-ZrB<sub>2</sub> can be ascribed to the formation of void-free composite by ensuring wettability through the process parameters employed.

### 3.3. Corrosion performance of AA8011-ZrB<sub>2</sub> in NaCl

The behaviour of AA8011 with and without ZrB<sub>2</sub> reinforcement in an environment of 3.5% NaCl was investigated using the Auto lab potentiodynamic polarization technique. Fig. 4 reveals the anodic and cathodic branch polarization curve of AA8011-ZrB<sub>2</sub> from where the corrosion density ( $I_{corr}$ ), corrosion rate (mm/yr), corrosion potential ( $E_{corr}$ ), and polarization resistance ( $\Omega$ ) was extrapolated by Tafel as summarized in Table 3. The result of the experiment shows a high corrosion rate of 4.61 mm/yr. The corrosion current density of the AA8011 was found to be high with the value of  $3.90 \times 10^{-4}$  A/cm<sup>2</sup>, this high density is due to the presence of the active negative Cl ion that diffuse to the unprotected metal surface thereby creating a pitting site of corrosion [32].

The influence of the inert nano insulated ZrB<sub>2</sub> was examined on the metal dissolution of AA8011 in a simulated chloride ion environment at ambient temperature. A shift in the direction of a reduced corrosion density was observed in Fig. 4 as the inclusion of ZrB<sub>2</sub> increases from 5 wt% to 20 wt% and the lowest density of  $6.54 \times 10^{-5}$  was achieved at 20 wt% inclusion. This is an indication that the presence of ZrB<sub>2</sub> has sufficiently blocked the possible susceptible site of corrosion initiation by reducing the density. Naturally, it is believed that metal surfaces are characterized with nanopores which might be probably invisible, these pores become explicitly exposed when in contact with an aggrieved deteriorating medium especially when not protected thereby creating rooms for cathodic reaction with a high density of vulnerable sites. The widespread of the inert ZrB<sub>2</sub> occupies the pore-spaces on the AA8011 metal surface and this invariably reduces the density of the susceptible site and hinders the continuous cathodic reaction. The successful discontinuity of the cathodic reaction establishes a

minimum rate of corrosion, and a high potential that corrosion would not occur. The above illustration was witnessed by the corrosion potential and the corrosion rate value obtained in Table 3. From the plot in Fig. 4 and Table 3, a high potential of about -1.4014 (V) that corrosion would occur with an associated high corrosion rate of 4.6129 mm/yr was observed with the unreinforced AA8011. However, the tendency of corrosion occurrence decreases with the addition of the insulated ZrB<sub>2</sub> and this retardation against corrosion attack increases with the weight percentage of the nano inclusion due to its extensive occupancy in volume proportion in the location of the active site and the barrier bridge against continuous cathodic reaction. Hence, the composites reinforced with 20 wt% was seen with the lowest potential of corrosion occurring of about -0.8792 V and the lowest corrosion rate of 0.5017 mm/yr.

A similar result has been reported by Fayomi et al., 2020 when the authors examined the corrosion behaviour of the reinforced AA8011 with nitride ceramic material and achieved a better corrosion resistance with an increase in the Si<sub>3</sub>N<sub>4</sub> addition. Moreover, the authors established the fact that the inability of AA8011 to regenerate its inherent passive protective thin film layer in the chloride medium which in turn lead to high exposure was responsible for the high corrosion density of the susceptible site. Hence, corrosion attacks become irresistible with a high corrosion rate. Likewise, several researchers have experimented with the impact of the ceramic nitride, borides, carbides, and oxides on the corrosion susceptibility of the aluminium alloys and their results show a significant increase in corrosion resistance [33,34].

The evidence of the pitting corrosion is shown by the SEM micrographs in Fig. 5, and the deterioration caused by the aggressive chloride anions was revealed in the form of pits and cracks. As seen on the micrograph, the unreinforced AA8011 was characterized by severe cracks and deep pitting due to the infiltration of the electrolyte (Cl<sup>-</sup>) that exposes the unprotected pore-space to more severe damages. The penetration of the chloride ion was retarded by the incorporation of the inert ZrB<sub>2</sub> and this reduces the cathodic reaction leading to less localized pitting and cracking impacts. This, therefore, means that the presence of the nano inclusion reduces the degree at which the electrolyte ion gain access to the metal surface. Moreover, the higher the percentage weight content of the reinforcing nano inclusion (ZrB<sub>2</sub>), the more surface protective coverage rendered to the unreinforced AA8011. This explains why no significant structural deformation was revealed on the surfaces of the composite with 15 wt % and 20 wt% ZrB<sub>2</sub>. The SEM micrographs revealed in Fig. 5 have further help to understand the mechanism behind the high corrosion rate of AA8011 despite its inherent passivation nature in the form of a thin-film oxide layer. The layers of the protective films are broken over time when in contact with the aggressive ion medium and before it could regenerate, the surface is exposed, and the corrosion process has been initiated.

Previously, Fayomi et al., 2020 reported that the extent of the uniform dispersion of the nano ceramic inclusion in the matrix of AA8011 determines the height of the protection rendered to the host alloy. Hence, high resistance of 7831.7  $\Omega$  at 20 wt% ZrB<sub>2</sub> was due to the wettability achieved.

Table 3  
Corrosion extrapolation of AA8011-ZrB<sub>2</sub>.

Specimen	Corrosion Potential (V)	Current Density (A/cm <sup>2</sup> )	L R <sub>p</sub> ( $\Omega$ )	Corrosion Rate (mm/yr)
AA8011 (as-cast)	-1.4014	$3.90 \times 10^{-4}$	137.48	4.6129
AA8011-5% ZrB <sub>2</sub>	-1.3238	$3.05 \times 10^{-4}$	152.65	4.2364
AA8011-10% ZrB <sub>2</sub>	-1.2117	$2.75 \times 10^{-4}$	607.66	3.4390
AA8011-15% ZrB <sub>2</sub>	-1.0983	$6.73 \times 10^{-5}$	5140.2	0.7083
AA8011-20% ZrB <sub>2</sub>	-0.8792	$6.54 \times 10^{-5}$	7831.7	0.5017

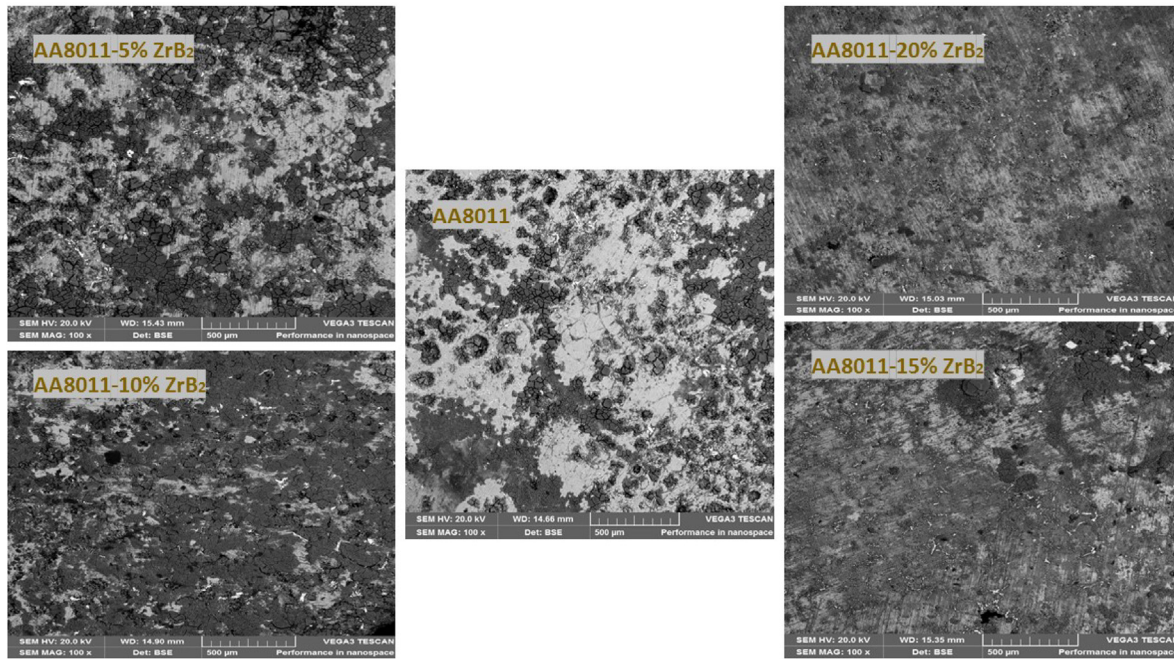


Fig. 5. SEM micrograph of the corroded surfaces in 3.5% NaCl.

#### 4. Conclusions

The microstructural adjustment and modification through the contribution of the reinforcement additives by the two-steps stir casting process has distinctively improved the structural properties and material stability of the aluminium AA8011. The fabrication of new crystallized AMMCs with a uniform dispersion of the reinforcement  $ZrB_2$  phase and excellent bonding structure yield the following progressive variation:

1. The percentage weight loss as a function of temperature was achieved using a thermal gravimetric analyzer (TGA) at the heating rate ranging from 30 C to 900 C in an inert nitrogen environment. Minimal weight loss of 0.11 mg was experienced by composite reinforced with AA8011-20%  $ZrB_2$ . This is an indication that the reinforced composite is more thermally stable than the AA8011 matrix and this assertion was affirmed by the differential thermal analysis (DTA) results. The DTA revealed the solid-liquid transition (melting point temperature) and the as-cast AA8011 was observed to melt at the endothermic peak of 661.0 C while the composite with AA8011-20%  $ZrB_2$  melted at 674.4 C.
2. The incorporation of the inert insulated  $ZrB_2$  material retard the free electron movement in the base primary AA8011. Hence, a decrease in the inherent electrical conductivity of AA8011 was experienced although the reduction was minimum. However, the resistivity behaviour of the developed composite was increased and 20 wt %  $ZrB_2$  was identified with high resistivity of  $4.42 \times 10^{-6} \Omega m$
3. The addition of Nanosized ceramic reinforcement in the AA8011 alloy by two-steps stir casting process amounted to a significant decrease in the corrosion rate of the developed composite in the aggressive saline environment. From the result of the corrosion analysis in 3.5% NaCl, AA8011-20%  $ZrB_2$  exhibited good corrosion resistance prowess with the lowest corrosion rate of 0.5017 mm/yr and high resistance of 7831.7  $\Omega$ .

#### CRediT authorship contribution statement

**J. Fayomi:** Conceptualization, Methodology, Formal analysis, Investigation, Data curation, Writing - original draft, Writing - review & editing, Visualization. **A.P.I. Popoola:** Resources, Supervision, Funding acquisition. **O.M. Popoola:** Software, Supervision. **O.S.I. Fayomi:** Conceptualization, Validation, Investigation, Writing - review & editing, Project administration. **E. Ajenifuja:** Software, Formal analysis.

#### Declaration of competing interest

The authors declare that they have no known competing financial interests or personal relationships that could have appeared to influence the work reported in this paper.

#### Acknowledgment

Appreciation to the Department of Chemical, Metallurgical, and Materials Engineering, Surface Engineering Research Laboratory, Centre for Energy and Electric Power of the Tshwane University of Technology, National Research Foundation South Africa, and Covenant University Nigeria for the supports and provision of equipment to execute this research

#### References

- [1] C.O. Ujah, A.P.I. Popoola, O.M. Popoola, V.S. Aigbodion, Enhanced tribology, thermal and electrical properties of Al-CNT composite processed via spark plasma sintering for transmission conductor, J. Mater. Sci. (2019), <https://doi.org/10.1007/s10853-019-03894-x>.
- [2] C.W. Kim, J.I. Cho, S.W. Choi, Y.C. Kim, C.S. Kang, The effect of alloying elements on thermal conductivity and casting characteristics in high-pressure die casting of aluminium alloy. Proceedings of 13th International Conference on Aluminium Alloys (ICAA13): TMS (The Minerals, Metals & Materials Society), 2012.
- [3] D. Ramesh, R.P. Swamy, T.K. Chandrashekar, Effect of weight percentage on mechanical properties of frit particulate reinforced al6061 composite, ARPN J

- Eng. Appl Sci 5 (1) (2010) 1819–2660.
- [4] M. Mariyappan, P. Sarangapani, G. Perumal, A. Sathiyamoorthi, Improvement in tribological behavior of aluminum 356 hybrid metal matrix composites. International Conference on Recent Advancement in Mechanical Engineering & Technology (ICRAMET'15), Journal of Chemical and Pharmaceutical Sciences ISSN (2015) 974–2115.
  - [5] N. Muralidharan, K. Chockalingam, I. Dinaharan, K. Kalaiselvan, Microstructure and mechanical behavior of AA2024 aluminium composites reinforced with in-situ synthesized ZrB<sub>2</sub> particles, J. Alloys Compd. 735 (2018) 2167–2174.
  - [6] G.R. Jinu, G. Karthikeyan, P. Vijayalakshmi, Development and mechanical properties analysis of aluminum LM14- MgO metal matrix composite using FEA, Concurr. Adv. Mech. Eng 2 (2) (2016) 20e32.
  - [7] J. Fayomi, A.P.I. Popoola, O.M. Popoola, Corrosion performance and thermal behaviour of AA8011 reinforced with hybrid nano ZrB<sub>2</sub>+Si<sub>3</sub>N<sub>4</sub> Particulates for Automobile Applications, Mater. Res. Express 6 (11) (2019) 1150e2.
  - [8] X. Zi-Yang, C. Guo-Qin, W. Gao-Hui, Y. Wen-Shu, L. Yan-Mei, Effect of volume fraction on microstructure and mechanical properties of Si<sub>3</sub>N<sub>4</sub>/Al composites, Trans. Nonferrous Metals Soc. China 21 (2011) 285–289.
  - [9] R.J. Kandam, D. Kumar, M. Sudharssanam, Badrinath R. Venkadesan, Investigation of mechanical properties on newly formulated hybrid composite aluminium 8011 reinforced with BaC and Al<sub>2</sub>O<sub>3</sub> by stir casting method, Int. J. Sci. Res. Develop 5 (1) (2017).
  - [10] S. Lal, S. Kumar, Z.A. Khan, Microstructure evaluation, thermal and mechanical characterization of hybrid metal matrix composite, Sci. Eng. Compos. Mater. (2018), <https://doi.org/10.1515/secm-2017-0210>.
  - [11] A. Karthikeyan, G.R. Jinu, Investigation on mechanical and corrosion behaviour of AA8011 reinforced with TiC and graphite hybrid composites, Mater. Res. Express 6 (10) (2019) 1065b5.
  - [12] S. Magibalan, K.P. Senthil, P. Vignesh, M. Prabu, A.V. Balan, N. Shivasankaran, Aluminium metal matrix composites – a review, Trans Adv Sci Techno (Tas-tonline) 1 (2) (2017) 1–6.
  - [13] P.O. Babalola, C.A. Bolu, A.O. Inegbenebor, O. Kilanko, S.O. Oyedepo, K.M. Odunfa, Producing AA1170 based silicon carbide particulate composite through stir casting method, Asian J Mater Chem (2017), <https://doi.org/10.14233/ajmc.2017. AJMC-P49>.
  - [14] T.G. Rambau, A.P.I. Popoola, C.A. Loto, T. Mathebula, M. Theron, Tribological and corrosion characterization of Al/(satellite-6+zirconium) laser alloyed composites, Int J Electrochemical Sci 8 (2013) 5515–5555.
  - [15] V.R. Rao, N. Ramanaiah, M.M.M. Sarcar, Tribological properties of aluminium metal matrix composites-AA7075 reinforced with titanium carbide (TiC) particles, Int J Adv Sci Techno 88 (2016) 13–26.
  - [16] J. Fayomi, A.P.I. Popoola, O.M. Popoola, O.S.I. Fayomi, Influence of zirconium diboride (ZrB<sub>2</sub>) on the physio-mechanical properties of high-grade AA8011 metal matrix composites, J Phys Conf Ser 1378 (3) (2019), 032044.
  - [17] K.R. Vasanth, R. Keshavamurthy, P.S. Chandra, Microstructure and mechanical behaviour of Al6061-ZrB<sub>2</sub> in-situ metal matrix composites, IOP Conf. Ser. Mater. Sci. Eng. 149 (2016), 012062, 587.
  - [18] B.M.M. Selvan, A. Veeramani, D. Muthukannan, Investigation of tribological behaviour of AA8011-ZrB<sub>2</sub> in-situ cast-metal-matrix composites, Mater. Technol. 52 (4) (2018) 451–457.
  - [19] E.W. Neuman, Elevated Temperature Mechanical Properties of Zirconium Diboride Based Ceramics, 2014.
  - [20] G. Gautam, A. Mohan, Effect of ZrB<sub>2</sub> particles on the micro-structure and mechanical properties of hybrid (ZrB<sub>2</sub> + Al<sub>3</sub>Zr)/AA5052 in-situ composites, J. Alloys Compd. 649 (2015) 174–183.
  - [21] B. Ravi, Fabrication and mechanical properties of Al7075-SiC-TiC hybrid metal matrix composites, Int J Eng Sci Invention 6 (10) (2017) 12–19.
  - [22] L.E.G. Cambronero, E. Sánchez, J.M. Ruiz-Roman, J.M. Jruiz-Prieto, Mechanical characterization of AA7015 aluminium alloy reinforced with ceramics, J. Mater. Process. Technol. (2003) 378–383.
  - [23] S.B. Hassan, V.S. Aigbodion, Effects of eggshell on the microstructures and properties of Al–Cu–Mg/eggshell particulate composites, J King Saud Univ – Eng Sci 27 (2015) 49–56.
  - [24] J. Fayomi, A.P.I. Popoola, O.M. Popoola, O.P. Oladajo, O.S.I. Fayomi, Tribological and microstructural investigation of hybrid AA8011/ZrB<sub>2</sub> -Si<sub>3</sub>N<sub>4</sub> nano-materials for service life improvement, Results Phys 14 (2019) 102469.
  - [25] J. Fayomi, A.P.I. Popoola, The assessment of the microstructural modification, corrosion response, and tribological behaviour of AA8011 reinforced nano ZrB<sub>2</sub> for life span enhancement in automobile application, J Bio- and Tribo-Corrosion 6 (2020) 9.
  - [26] S.Y. Lee, I.A. Kang, G.H. Doh, W.J. Kim, J.S. Kim, H.G. Yoon, Q. Wu, Thermal, mechanical, and morphological properties of polypropylene/clay/wood flour nanocomposites, Express Polym. Lett. 2 (2) (2008) 78–87.
  - [27] S.M. Krishna, T.N. Shridhar, L. Krishnamurthy, Experimental investigations on thermal analysis and thermal characterization of Al 6061-SiC-Gr hybrid metal matrix composites, Int. J. Mater. Sci. 5 (2) (2015) 54.
  - [28] R.N. Prabha, E.R.J. Dhas, Effect of TiC and MoS<sub>2</sub> reinforced aluminium metal matrix composites on microstructure and thermogravimetric analysis, Rasayan J. Chem 10 (3) (2017) 729–737.
  - [29] J. Fayomi, A.P.I. Popoola, O.M. Popoola, O.S.I. Fayomi, The appraisal of the thermal properties, electrical response, and corrosion resistance performance of AA8011 reinforced Nano Si<sub>3</sub>N<sub>4</sub> for automobile application, J. Alloys Compd. (2020), <https://doi.org/10.1016/j.jallcom.2020.156679>.
  - [30] M.M.M. Mohammed, O.A. Elkady, A.W. Abdelhameed, Effect of alumina particles addition on physico-mechanical properties of al-matrix composites, Open J. Met. 3 (2013) 72–79.
  - [31] R. Cao, J.X. Jiang, C. Wu, X.S. Jiang, Effect of addition of Si on thermal and electrical properties of Al-Si-Al<sub>2</sub>O<sub>3</sub> composites, in: Proceedings of 2017 Global Conference on Polymer and Composite Materials (PCM 2017): IOP Conf. Series: Materials Science and Engineering, 2017, 012001, <https://doi.org/10.1088/1757-899X/213/1/012001>.
  - [32] R.T. Loto, P. Babalola, Corrosion polarization behaviour and microstructural analysis of AA1070 aluminium silicon carbide matrix composites in acid chloride concentrations, Cogent Eng 4 (2017) 1.
  - [33] M. Sambathkumar, P. Navaneethakrishnan, K. Ponappa, K.S.K. Sasikumar, Mechanical and corrosion behavior of Al7075 (hybrid) metal matrix composites by two step stir casting process, Lat. Am. J. Solid. Struct. (2016), <https://doi.org/10.1590/1679-78253132>.
  - [34] K. Bandil, H. Vashisth, S. Kumar, L. Verma, A. Jamwal, D. Kumar, N. Singh, K.K. Sadasivuni, P. Gupta, Microstructural, mechanical and corrosion behaviour of Al-Si alloy reinforced with SiC metal matrix composite, J. Compos. Mater. 53 (28–30) (2019) 4215–4223.